Article

Not peer-reviewed version

Optimization of rebar usage and sustainability based on special-length priority: A case study on mechanical couplers in diaphragm wall

Daniel Darma Widjaja , Lwun Poe Khant , Sunkuk Kim , Kil Yong Kim *

Posted Date: 11 December 2023

doi: 10.20944/preprints202312.0703.v1

Keywords: sustainability impact, mechanical coupler, diaphragm wall, special length

Preprints (www.preprints.org) | NOT PEER-REVIEWED | Posted: 11 December 2023 doi:10.20944/preprints202312.0703.v1

Article

Optimization of Rebar Usage and Sustainability Based on Special-Length Priority: A Case Study on Mechanical Couplers in Diaphragm Wall

Daniel Darma Widjaja, Lwun Poe Khant, Sunkuk Kim and Kil Yong Kim *

Department of Architectural Engineering, Kyung Hee University, Yongin-si 17104, Republic of Korea; danieldarma@khu.ac.kr (D.D.W.), lwunpoekhant@khu.ac.kr (L.P.K.), kimskuk@khu.ac.kr (S.K.)

* Correspondence: stsata2937@khu.ac.kr; Tel.: +82-31-201-3685

Abstract: The construction industry generates significant CO_2 emissions, and rebar is a major contributor to this environmental impact. Extensive research has been conducted to address this issue. Recent advancements have introduced algorithms to reduce rebar waste and consumption, demonstrating the feasibility of achieving near-zero rebar cutting waste (N0RCW) by considering special-length rebars. However, conventional lap splices, the most common rebar joint method, consistently consume excessive rebar quantities despite extending beyond their mandated zones. Conversely, couplers eliminate rebar lengths required for lapping splices, reducing the usage of rebar. Applying special lengths and couplers in heavily loaded structures like diaphragm walls can significantly reduce rebar usage and cutting waste, consequently reducing CO_2 emissions and associated costs. This study aims to optimize rebar consumption and sustainability in diaphragm wall structures by integrating mechanical couplers with a special-length rebar approach. A case study confirmed a substantial reduction in purchased rebar usage (17.95% and 5.38%) and carbon emissions (15.24% and 2.25%) compared to the original design and previous study, respectively. Broadly implementing the proposed method across various buildings and infrastructure projects could further multiply these benefits, fostering the achievement of SDGs adopted by the United Nations for sustainable construction.

Keywords: sustainability impact; mechanical coupler; diaphragm wall; special length

1. Introduction

Steel reinforcement bar has a high embodied carbon footprint, about 9.2 times that of concrete [i], making it one of the major contributors to greenhouse gases (GHG) emissions. The US Environmental Protection Agency [ii] denotes that GHGs comprise 79.4% CO_2, 11.5% CH_4 (methane), 6.2% N_2O (nitrous oxide), and 3% fluorinated gases. It is reported that in 2020 the global consumption of concrete reached 14 billion m^3 [iii]. This amount corresponds to 1.078 billion tons of rebar, a cutting waste of 53.9 million tons, wasting 188.92 million tons of CO_2. Improperly managed cutting waste can end up in landfills, occupying valuable limited space of landfill and contributing to the production of landfill gas (LFG). LFG mainly constituted 40-50% CO_2 and 50-60% CH_4 [iv], with trace amounts of H_2S (hydrogen sulfide) [v]. Methane is a powerful GHG and is estimated to have a GWP (Global Warming Potential) of 27-30 over 100 years [2]. It has been discovered that rebar and concrete can significantly contribute to acid rain formation [vi]. Acid rain forms when harmful gases such as sulfur dioxide (SO_2) and nitrogen dioxide (NO_2) react with water vapor in the atmosphere [vii]. Acid rain causes significant harm to the environment, particularly to the soil. In addition, steel and rebar production may contribute to mercury emissions besides carbon emissions, leading to ecotoxicity [viii]. Mercury emissions can adversely impact the environment by polluting water bodies, harming wildlife, and posing a risk to human health.

Conventional lap splicing, the prevailing method for connecting rebars, is also a major contributor to rebar waste and CO_2 emissions in the construction industry, especially in large-scale projects like diaphragm walls, due to the long overlapping lengths of rebar required. Lap splice-based rebar waste depends on rebar diameter, required lap length, and cutting pattern.

Preprints (www.preprints.org) | NOT PEER-REVIEWED | Posted: 11 December 2023 doi:10.20944/preprints202312.0703.v1

One challenge in reducing rebar waste is adhering to lap splice regulations mandated by building codes. Lap splice length is typically derived from the bonding strength between concrete and steel rebar, considering the safety factor. Thus, the structural design provides a safe sufficient lap splice length. However, the lap splice position or region regulations mandated by the building codes and stock-length rebar usage restrict the reduction of rebar usage and cutting waste as per various studies [ix, x, xi, xii], ranging from 7.2% to 10.6%, exceeding the common range of 3-5% [xiii]. Nonetheless, it is difficult to adhere to these regulations on-site, and thus lap splice positions are often not followed in practice [xiv]. This approach continuously consumes a greater quantity of rebars, even when not adhering to mandated regulations. Researchers proposed special length rebars as one of the solutions to the high rebar consumption and waste issue. Investigations confirmed that special-length rebar enables further reduction in cutting waste to below 3% [xv, xvi].

Massive substructures such as diaphragm walls could illustrate the issue. The case study found that purchasing stock-length rebars for reinforcement in a total of 293 diaphragm wall panels resulted in 2173 tons (9.62%) of cutting waste [15], as large-diameter rebars (32 mm and 40 mm) were required to resist the massive lateral forces such as an earthquake in addition to the pressure of soil. The study additionally revealed that the utilization of special length rebars in diaphragm walls results in the consumption of 19,582 tons of rebar and the generation of 0.77% of cutting waste. Consequently, the adverse environmental impact due to high rebar usage remains evident. Furthermore, the ACI building code [xvii] prohibits lap splices for rebar sizes with a diameter of 36 mm and larger due to long overlapping lengths. Mechanical couplers can be used instead of lap splices to effectively transfer the tensile strength of rebar while maintaining structural integrity and stability. Couplers eliminate the need for lap splices, which further reduces required rebar, associated cutting waste, and environmental impact.

Prior studies have primarily focused on columns [xviii, xix], beams [18], and shear walls [10] for rebar cutting waste optimization, neglecting an essential structural component: diaphragm walls. Diaphragm walls play a pivotal role as the foundation backbone of building structures [xx], serving to connect various structural elements. Comprising multiple wall panels with similar reinforcement, the unique characteristic of diaphragm wall rebar lies in its prefabrication into rebar cages. **A significant reduction in rebar usage and carbon emissions is expected by performing detailed reinforcement design and optimizing for special lengths.**

1.1. Rebar usage and cutting waste issues

Global concrete volume reached 14 billion m^3 in 2020 [3]. Converting this amount with a rebar-to-concrete consumption ratio of 0.077 tons/m^3 [1] indicates that 1.078 billion tons of rebar are used. Assuming a 5% cutting waste rate, this results in 53.9 million tons of rebar-cutting waste and 188.92 million tons of carbon emission. Cutting steel reinforcement bars (rebar) is unavoidable in reinforced concrete (RC) structure construction and generates cutting waste and considerable carbon emissions [xxi]. Considering a rebar price of USD 900/ton [xxii], a unit of rebar-carbon emissions of 3.505-ton-CO_2/ton [xxiii], and a carbon price of USD 75/ton-CO_2 [xxiv], implies a loss of USD 62.68 billion for the industry. This condition urges stronger efforts to reduce rebar usage and cutting waste, contributing to environmental sustainability.

Rebar usage and cutting waste issues have been the concerns of the Sustainable Development Goals (SDGs) [xxv] created by the United Nations in 2015, especially SDGs 12, 13, and 15. SDG 12 aims to ensure sustainable consumption and production patterns; SDG 13 aims to take serious action to combat climate change and its impacts; finally, SDG 15 aims to protect and restore land, as well as halt land degradation. Reducing rebar usage and its impact will accelerate the achievement of the SDGs in the civil engineering and construction sector.

Most studies conducted rebar waste minimization on stock length rebars [xxvi, 10, 11, 12]. Some investigations [9, 10] explored the lap splice position optimization with stock-length rebar to reduce rebar cutting waste. These approaches, however, still produced a high cutting waste rate. Special-length rebar concepts are then introduced for cutting pattern combinations and have been confirmed to significantly reduce cutting waste [13, 18, xxvii]. Special lengths can be customized in 0.1 m intervals

Preprints (www.preprints.org) | NOT PEER-REVIEWED | Posted: 11 December 2023 doi:10.20944/preprints202312.0703.v1

and have certain order requirements such as maximum and minimum special lengths, minimum ordered quantity, and preorder time. Rachmawati et al. [15] proposed a three-step algorithm to minimize rebar cutting waste in diaphragm walls by considering special lengths and lap splice position adjustments. The algorithm generated 0.77% rebar cutting waste from 293 panels of diaphragm wall, saving 10,399 tons of CO_2 emissions and USD 3,480,108 in costs.

1.2. Mechanical couplers

The use of mechanical couplers has increased in construction due to their advantages which solve the limitations of conventional lap splices. Table 1 summarizes the limitations of conventional lap splices identified by various studies. Furthermore, several investigations [xxviii, xxix, xxx] have emphasized that the application of lap splices may over-reinforce the structural section, reduce ductility, and alter the deformation capacity.

Table 1. Conventional lap splice limitations.

Author(s)	Description
Singh et al. [xxxi]	Time-consuming in design and installation. Increased rebar congestion probability. Increased amount of rebar used.
Chiari and Junior [xxxii]	Limited use in structural restoration. Limited allowable rebar diameters for splicing.
Shokrzadeh et al. [28]	Increased rebar consumption and cost, especially for bars with a diameter greater than 30 mm. Rebar congestion issue due to lap splicing.
Damsara and Kulathunga [xxxiii]	Rebar congestion issue due to lap splicing. Significant rebar waste due to the longer lap lengths required for larger diameter rebars.

A mechanical coupler, also known as a mechanical splice or rebar coupler, is a device used for connecting two rebars, eliminating the lapping length, and ensuring the structural stability and strength of RC structures. In seismic applications, the coupler length should be less than 15 times the rebar diameter [xxxiv]. Rebars with different diameters can be connected laterally or vertically by using couplers. Mechanical coupler utilization can significantly reduce rebar congestion and also offer prefabrication of reinforcement on-site for precast concrete structures [xxxv]. Mechanical couplers have been shown to offer several benefits [31]: (1) reduced rebar congestion, (2) significant reduction in rebar waste and consumption, (3) effective control of concrete crack propagation, (4) improved structural continuity between bars, ensuring better integrity, (5) reduced labor required and construction costs, and (6) feasibility of connecting rebars of different lengths and diameters.

In the current construction industry, various types of couplers are employed. The five types of couplers which are readily available are (1) shear screw couplers, (2) headed bar couplers, (3) grouted sleeve couplers, (4) threaded couplers, and (5) swaged couplers [34]. The most prevalent type is the threaded coupler, characterized by its short length and ease of installation [xxxvi, xxxvii]. Four types of threaded couplers are commonly used: parallel threaded couplers (PTC), taper threaded couplers (TTC), upset-headed couplers (UHC), and rib thread couplers (RTC) [xxxviii].

1.3. Research objective

Rapid urbanization and the construction of high-rise buildings are reducing the availability of urban land [xxxix]. This has led to an increase in the construction of underground and buried structures in metropolitan cities [xl], such as diaphragm walls. Population growth and urbanization are driving demand for construction, which is depleting natural resources used in construction materials and harming the environment [xli].

Preprints (www.preprints.org) | NOT PEER-REVIEWED | Posted: 11 December 2023 doi:10.20944/preprints202312.0703.v1

Given the considerable demand for steel rebars in diaphragm wall construction, it represents an exemplary case study for optimizing rebar usage and environmental sustainability. The primary objective of this research is to assess the effectiveness of mechanical couplers in optimizing rebar usage and cutting waste of diaphragm walls and improving sustainability by integrating mechanical couplers with a special-length priority approach. A comprehensive analysis of rebar usage and cutting waste, considering the environmental and economic implications, is presented in this research. To identify the effectiveness and novelty of the proposed method, a comparative analysis will be undertaken against the conventional lap splice method of the original design and the recent study [15]. This comparison will encompass rebar usage, cutting waste, cost, and the CO_2 emissions associated with cutting waste. Furthermore, this research will analyze the cost comparison between using couplers and the conventional method of overlapping rebar. This research provides the construction industry with new insights into optimizing rebar usage and sustainability while maintaining structural integrity and addressing the environmental impact of rebar. Furthermore, it also accelerates sustainable and green construction practices and the achievement of the Sustainable Development Goals (SDGs).

2. Characteristics of diaphragm wall

Diaphragm walls are underground reinforced concrete structures that extend vertically or at a slight angle, commonly used in underground construction, foundation systems, and retaining walls to provide lateral support. Diaphragm walls resist lateral forces from soil and water pressure, and transfer lateral loads induced by seismic events or other dynamic forces to the foundation of a building [20, 40]. A diaphragm wall system is generally composed of multiple wall panels. Main vertical rebars resist vertical and bending loads generated by lateral loads from soil, water pressure, and seismic activity. Horizontal (space) rebars distribute loads evenly along the length of the wall. Transverse shear, shear link, or tie reinforcement resists shear forces caused by lateral loads.

Diaphragm walls require a substantial amount of steel reinforcement bars to withstand lateral soil forces. This reinforcement is prefabricated into rebar cages and divided into three or more sections depending on the wall's depth. Fabricated cages are inserted section by section into the excavated ground. Starter bars anchor the diaphragm wall reinforcement at every floor slab to ensure structural integrity. A typical diaphragm wall panel consists of two rebar cages. Each rebar cage can be divided into three groups of reinforcement: main vertical rebars, space bars, and horizontal ties or links. Additional rebars for various purposes, such as spacers, fixing rebars, stiffeners, hanging bars, suspension hooks, and lifting rebars, are also incorporated to strengthen the cage and aid in the installation process. The main vertical rebars in the cage are held in position by horizontal links such as EX-links and C-links, which serve a similar function to hoops in column reinforcement. Figure 1 illustrates the rebar arrangement of the rebar cage.

Diaphragm wall construction typically follows four steps: (1) constructing a guide wall, (2) excavating the soil and filling the space with slurry, (3) installing rebar cages, and (4) pouring concrete using a tremie pipe. The guide wall is temporarily constructed to ensure the alignment of wall continuity and to assist in the installation of rebar cages. The dimensions of a wall panel depend on geological conditions and structural designs [40]. Diaphragm wall construction begins with the construction of primary wall panels, followed by secondary panels. Special joints with water stop connect the wall panels, with the specific type of joint varying depending on the contractor's preference or excavating equipment used.

Preprints (www.preprints.org) | NOT PEER-REVIEWED | Posted: 11 December 2023 doi:10.20944/preprints202312.0703.v1

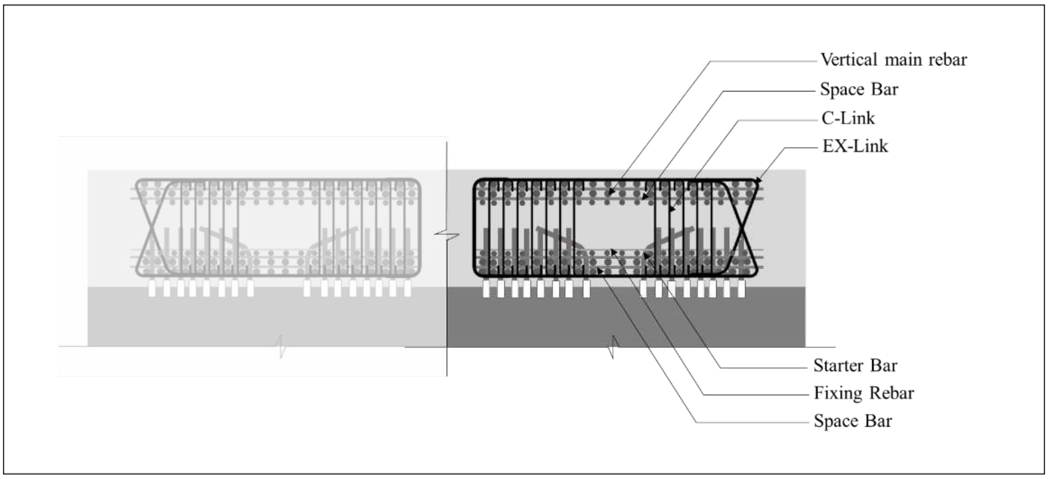

Figure 1. Rebar arrangement of a rebar cage

3. Methodology

Figure. 2 illustrates the flowchart of the proposed study. This outlines the process and validation procedure of our proposed approach, analyzing the impact of mechanical rebars on diaphragm wall rebar consumption.

Stage 1: Collect structural analysis results to obtain information about the location of structural members and rebar properties, including bar length, diameter, shape, quantity, and location.

Stage 2: Analyze the rebar arrangement within a diaphragm wall panel.

Stage 3: Create a Building Information Modeling (BIM) structural model and apply BS shape codes to retrieve the rebar list.

Stage 4: Implement a mechanical coupler-based special length rebar minimization algorithm on vertical main rebars.

Stage 5: Combine all the remaining rebars in a cutting pattern optimization algorithm using special lengths.

Stage 6: Analyze rebar consumption, rebar cutting waste, carbon emissions, and related costs to validate the proposed algorithm. Then compare the results of the proposed algorithm to those of the original design, which used the conventional lap splice method, with stock length rebars, and to the findings of the previous study [15], which also employed the lap splice method and incorporated special length rebars. Consequently, the impact of couplers is investigated through rebar cutting waste, costs, and generated amount of CO_2 emissions.

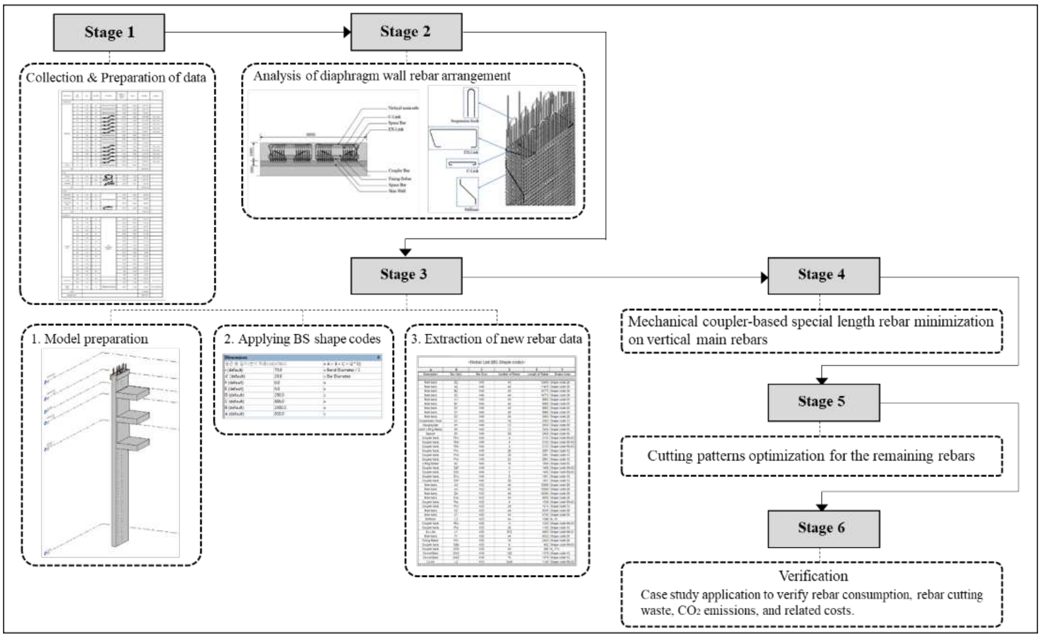

Figure 2. Flowchart of the methodology.

3.1. Mechanical coupler-based special-length-priority optimization algorithm

The objectives and constraints for this study have been established for the optimization of special lengths considering mechanical couplers. The objective is to minimize rebar cutting waste to less than 1% by incorporating special lengths and couplers for the main vertical rebars. The constraints for the special length order include a minimum length of 6 meters, a maximum length of 12 meters, a minimum ordered quantity of 50 tons for each special length, and a pre-order lead time of two months [13].

Since the rebar cage of the diaphragm wall is arranged with rebars of different diameters, the deeper the wall panel, the smaller the rebar, the total length is calculated by combining all the rebars with the same diameter that are arranged in the same layer, as shown in Equation (1), which is adopted from the study by Rachmawati et al. [15].

$$L_{total} = \sum_{i=1}^{l} L_{rebar\_i} \tag{1}$$

in which, L_{total} is the total length of wall rebar in the same diameter; and L_{rebar_i} is the length of rebar i.

To obtain the number of required rebar in each total length, the continuous total rebar length is divided by the optimal reference length as in Equation (2), adopted from the study by Rachmawati et al. [15]. The optimal reference length is assumed to be 12 m in this study. The generated number is rounded up for a whole number.

$$n_{rebar} = \left\lceil \frac{L_{total}}{L_{ref}} \right\rceil \tag{2}$$

in which, n_{rebar} is the number of required rebars; and L_{ref} is the optimal reference length available in the market.

Then, to determine the special length of the rebar, Equation (3) is used considering the total length, the number of rebars required, and the gap between the threaded rebars. A threaded coupler typically includes a gap between the rebars to facilitate installation in case of misaligned threads and for grouting purposes [xlii]. To obtain the exact length, this gap must be deducted from the rebars. As illustrated in Figure 3, half of the gap is subtracted from the end rebar, while the entire gap is subtracted from the middle rebar. Since the special length is ordered in 0.1 m increments, the generated value is rounded up to one decimal place.

$$L_{special} = \left\lceil \frac{L_{total}}{n_{rebar}} - \frac{s}{2} \right\rceil \text{ for end rebar, } \left\lceil \frac{L_{total}}{n_{rebar}} - s \right\rceil \text{ for middle rebar} \tag{3}$$

in which, $L_{special}$ is the special length; and s is the space between the threaded rebars.

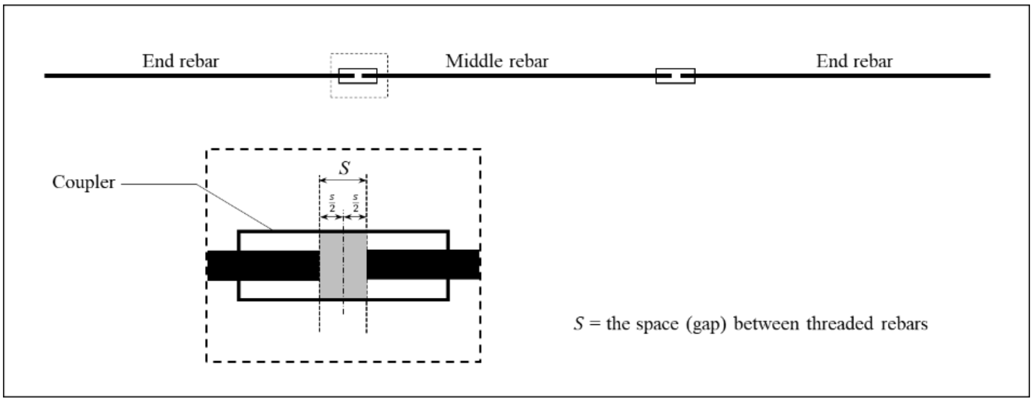

Figure 3. Illustration of end rebar and middle rebar.

3.2. Cutting pattern optimization algorithm

After special lengths are generated from the optimization of main rebars considering the couplers, all the remaining rebars are combined into special length cutting patterns, which produce the minimum cutting waste. Equation (4) is adopted from the study by Lee et al. [13] for the minimization of rebar cutting waste.

$$Minimize\ f(X_i) = \sum_{i=1}^{N} \frac{L_{spi}n_i - l_i n_i}{L_{spi}n_i} \tag{4}$$

in which, L_{spi} is the special length cutting pattern; l_i is the length of cutting pattern i obtained by combining required lengths; and n_i represents the number of rebar combinations with the same cutting pattern i.

4. Case study and Verification

4.1. Case study application

The proposed study was verified on the diaphragm wall of an interchange station, provided by the shop drawing set of a primary wall panel. The case diaphragm wall was comprised of multiple panels, including 293 primary wall panels, each measuring 6 m in length and 1m in width. The overall depth of the panel is 37.58 m; 31.08 m underground and 6.5 m above the ground level. All the wall panels were connected to the three floors of the interchange station: B2 concourse structural floor level, B1 subway structural floor level, and subway roof structural floor level. The depth of each floor slab is 1200 mm. Skin walls with 300 mm thickness were located between each floor. In this case study project, high tensile bar grade 500 MPa was employed for all the reinforcement. In addition, the diameter of the high tensile rebar symbolized as 'H' in the shop drawings, was also adopted in this study. The attributes of the case study diaphragm wall panel are summarized in Table 2.

Preprints (www.preprints.org) | NOT PEER-REVIEWED | Posted: 11 December 2023 doi:10.20944/preprints202312.0703.v1

Table 2. Attributes of the diaphragm wall panel.

Description	Contents
Length of D-wall	6 m
Width of D-wall	1 m
Overall depth of D-wall	37.58 m
Thickness of skin wall	300 mm
Depth of floor slab	1200 mm
Top concrete cover	100 mm
Bottom concrete cover	200 mm
Strength of rebars	SHD500
Concrete strength	24 MPa
Length of ordered rebar, l_{order} (m)	$6 \le l_{order} \le 12$

The case wall panel was reinforced with two similar rebar cages, each comprised of four rebar cage sections, as demonstrated in Figure 4(b). The reinforcement comprised vertical main rebars, horizontal EX-links, C-links, and additional rebars for lifting and aligning purposes. In each cage section, vertical main rebars were held in place by two EX-links. C-links anchored main rebars by sandwiching the EX-links. The 1st cage section employed six layers of main rebars which were separated by space bars, as shown in Figure 1. Stiffeners were used to strengthen the cage section and to prevent the cage from deformation. Starter bars were used to anchor the floor reinforcement to the rebar cages and were separated by fixing rebars to maintain the positions. For the lifting process, hanging bars and lifting bars were used for the lower cages from second to fourth, and suspension hooks were additionally employed for the first cage section.

The rebar marks from the original shop drawing were used. The letter in the rebar mark indicates the rebar layer and the number indicates the location of the rebar. As shown in Figure 4(b), the rebar mark "A1" indicates the vertical rebar in layer A of the 1st rebar cage section. The rebar layers A and D extended along the rebar cage from the 1st to the 4th section, while layers B and E were located only in the 1st and 2nd sections. The mechanical coupler-based special-length-priority optimization algorithm was applied to the vertical main rebars of the diaphragm wall panel, and all the remaining rebars were optimized in cutting patterns. The rebar layers C and F, located in the upper two sections were much smaller than the main rebars in both length and diameter, so they were included in the remaining rebars.

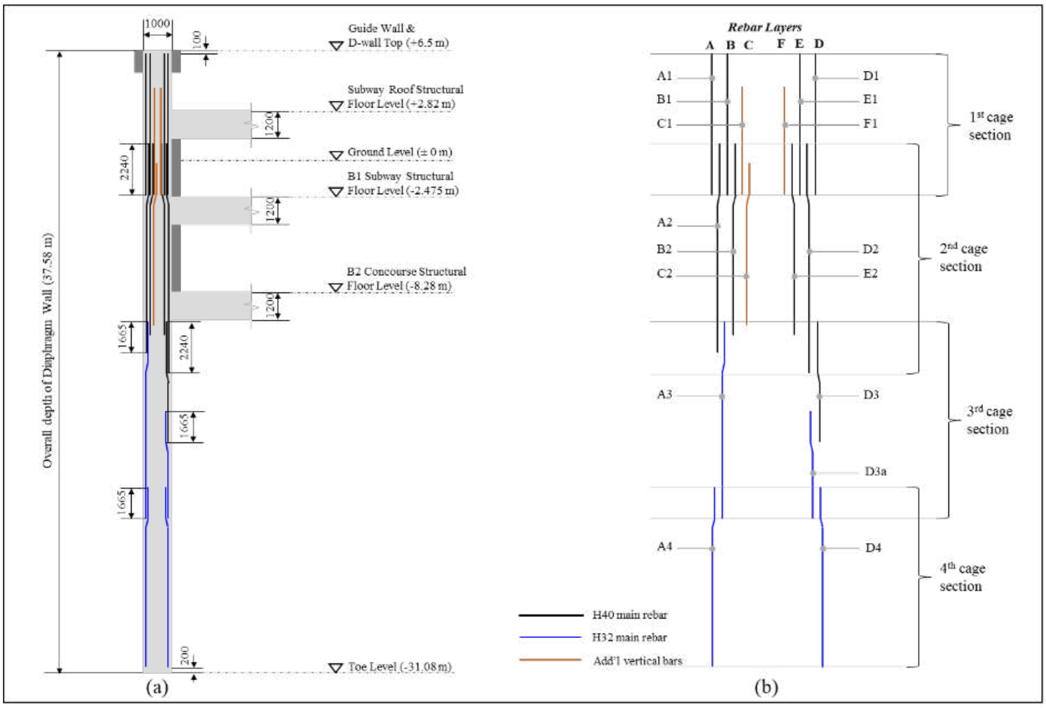

Figure 4. Vertical rebar arrangement of a diaphragm wall panel. (a) Cross-section. (b) Rebar cage sections. (Adapt from: Rachmawati et al. [4]).

Regarding the coupler usage, this study considered rib thread couplers, which generally consist of a cylindrical sleeve with threads onto which rebar ends are securely threaded and fastened with nuts (see Figure A1 in the Appendix). Table A1 in the Appendix provides the dimensions of threaded rebar couplers by Tokyo Tekko [xliii]. As shown in Figure A1, the coupler and threaded rebar have a gap between the threads, enabling construction even if the threads are misaligned. The gap is typically 20 mm for rebar sizes H16 to H29 and 30 mm for rebar sizes above H32 [42]. The coupler also provides a permissible tolerance for the rebar length inserted in the center, ensuring rebar connection even if the threaded rebars have a cutting length error.

4.1.1. Mechanical coupler-based special-length rebar minimization on main vertical rebars

The case application was conducted according to the stages described in the flowchart of the methodology, Figure 2. First and foremost, fundamental information about the diaphragm wall panel and its reinforcing bars was gathered from the case study project shop drawings. The original rebar list for the diaphragm wall is displayed in Appendix Table A2. Subsequently, a structural BIM model was created after analyzing the arrangement of rebar within the diaphragm wall and eliminating the lap lengths since the proposed study considered mechanical couplers. In addition, all rebars in the model were assigned BS shape codes. The revised rebar list obtained from this model is presented in Appendix Table A3, serving as the primary data source for this study.

The main vertical rebars of layers A, B, D, and E, as shown in Figure 4(b), were optimized in special lengths considering mechanical couplers instead of lap splices. Equations (1) to (3) were used to calculate the special length for the main rebars. In rebar layer A, H40 and H32 rebars were used as main vertical rebars. The optimization was conducted individually on the same diameter rebars. Therefore, rebars A1 and A2 were combined as the total length and divided by the optimal reference length of 12 m, resulting in the number of required rebars. Then the total length was again divided by the number of rebars to obtain the exact required length of rebars that are connected by couplers. Additionally, since a minimum of 30 mm gap was suggested between the threads for couplers' sizes above H32 [42], 15 mm was subtracted from each end rebar and 30 mm from each middle rebar for the required lengths. Table 3 summarizes the results of the mechanical coupler-based special length rebar minimization according to rebar layers. It was observed that rebar D3 was reduced from rebar layer D due to the minimization algorithm.

Table 3. Mechanical coupler-based special length rebar minimization on vertical main rebars.

Bar mark	Bar size (mm)	Unit weight (kg/m) [xliv, xlv]	No. of rebar	Required length (m)	Special length (m)	Required rebar quantity (ton)	Ordered rebar quantity (ton)	Loss rate (%)
A1	H40	9.864	40	9.010	9.1	3.555	3.590	0.99%
A2	H40	9.864	40	8.995	9.0	3.549	3.551	0.06%
B1	H40	9.864	40	8.685	8.7	3.427	3.433	0.17%
B2	H40	9.864	40	8.685	8.7	3.427	3.433	0.17%
E1	H40	9.864	40	8.685	8.7	3.427	3.433	0.17%
E2	H40	9.864	40	8.685	8.7	3.427	3.433	0.17%
D1	H40	9.864	40	11.010	11.1	4.344	4.380	0.81%
D2	H40	9.864	40	10.995	11.0	4.338	4.340	0.05%
A3	H32	6.313	40	9.585	9.6	2.420	2.424	0.16%
A4	H32	6.313	40	9.600	9.6	2.424	2.424	0.00%
D3a	H32	6.313	40	7.585	7.6	1.915	1.919	0.20%
D4	H32	6.313	40	7.600	7.6	1.919	1.919	0.00%
						38.172	38.279	0.28%

4.1.2. Cutting patterns optimization for the remaining rebars

Consequently, the remaining rebars in the diaphragm wall panel's rebar cage were combined in cutting pattern optimization using special lengths to generate minimal rebar cutting waste. Table 4 provides the results of cutting pattern optimization. From the table, the available market lengths of 12 m and 11 m were found to be the most efficient lengths for H32 and H13 rebars, respectively, in terms of minimizing cutting waste. However, since special lengths are purchased in 0.1 m intervals, these lengths were considered to be special lengths for the purpose of this study.

Table 4. Cutting pattern optimization for the remaining rebars.

Bar size (m)	Unit weight (kg/m) [44, 45]	Special length (m)	No. of rebar	Required rebar quantity (ton)	Ordered rebar quantity (ton)	Loss rate (%)
H40	9.864	10.3	51	5.129	5.182	1.01%
H32	6.313	12	4	0.302	0.303	0.41%
H25	3.854	10.6	65	2.600	2.655	2.08%
H20	2.466	9.6	513	12.040	12.145	0.86%
H16	1.560	8.2	38	0.484	0.486	0.34%
H13	0.995	11	383	4.155	4.192	0.87%
				24.711	24.963	1.01%

4.1.3. Analysis of the results by the algorithm

Figure 5(a) demonstrates the original arrangement of the main rebars; 1st and 2nd cage sections were arranged with H40 rebars. The 3rd cage section included both H40 and H32, in which bar mark D3 rebar was H40, and the rest were H32. The 4th cage section was arranged with H32 rebars. After special length rebar minimization based on mechanical couplers, the rebar cage was arranged with new special length rebars in each layer, as demonstrated in Figure 5(b). In rebar layer D, the number of rebars was reduced from three to two.

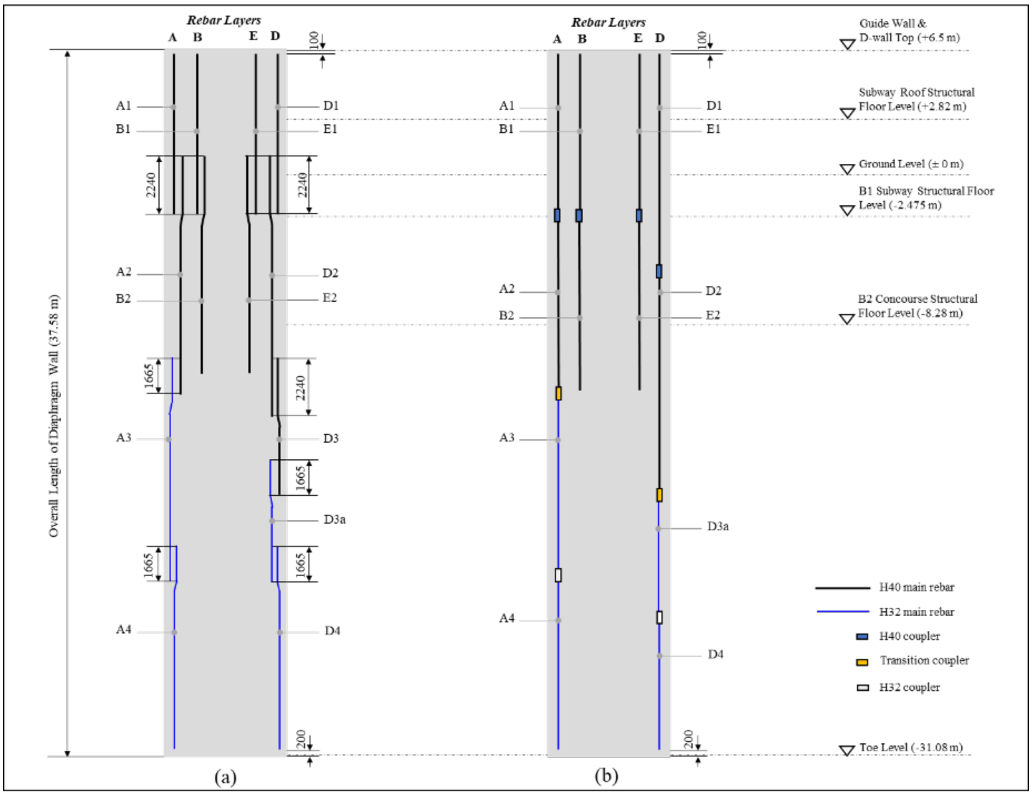

Figure 5. Diaphragm wall vertical rebar arrangement. (a) Before special length optimization. (b) After special length optimization.

Table 5 summarizes the required rebar quantity, ordered rebar quantity, and cutting waste after applying the proposed algorithm. The unit weights of rebars (H20, H16, and H13) are slightly different for these three cases. In the original case and the previous study [15], the unit weight of each rebar size was obtained from the information provided in the case study project. However, in the coupler case, both the rebars and couplers were purchased from the same company. Therefore, the unit weights were obtained from the company's specifications [44, 45]. It has been confirmed that the proposed algorithm considering mechanical couplers only generated 0.358 tons of rebar cutting waste with a 0.57% loss rate (less than 1%) in one diaphragm wall panel.

Table 5. Rebar quantities and cutting waste after applying the proposed algorithm (one panel).

Description	H40	H32	H25	H20	H16	H13	Total
Required quantity (ton)	34.623	8.981	2.600	12.040	0.484	4.155	62.884
Ordered quantity (ton)	34.774	8.990	2.655	12.145	0.486	4.192	63.241
Cutting waste (ton)	0.151	0.009	0.055	0.105	0.002	0.037	0.358
Loss rate (%)	0.43%	0.10%	2.08%	0.86%	0.34%	0.87%	0.57%

 doi:10.20944/preprints202312.0703.v1

4.2. Verification of the algorithm

The calculation was expanded to 293 panels of diaphragm wall. To verify the effectiveness of the algorithm, rebar quantities by the proposed algorithm were compared to the original case and the previous study by Rachmawati et al. [15] in terms of rebar quantities, carbon quantities, and associated costs. Since all the rebar length necessary for overlapping was eliminated, rebar usage for one panel was reduced by 17.95% from the original case which employed conventional lap splices and stock length rebars. The rebar quantities of the original case are shown in Appendix Table A4.

Table 6 shows the rebar quantities of the original case, the previous case, and the coupler case. The RCW rate of the original case was 9.62%, while the previous study and the coupler case achieved N0RCW by 0.77% and 0.57% respectively.

Table 6. Rebar quantities of the original case, the previous case, and the coupler case (293 panels).

Description	Required quantity (ton)	Ordered quantity (ton)	Cutting waste (ton)	Loss rate (%)
Original case	20,409.74	22,582.65	2172.91	9.62%
Previous case [15]	19,432.05	19,582.36	150.31	0.77%
Coupler case	18,424.88	18,529.69	104.81	0.57%

The rebar quantities were converted into carbon emissions to analyze the differences between each case. The carbon emission factors of rebar and coupler were referenced and interpolated based on the data from the study by Ghayeb et al. [23]. The factor of 3.505 ton-CO2 per rebar ton was used to calculate the carbon quantity of rebars. The carbon emission of the H32 coupler was 19.490 kg-CO2-e/pcs and that of the H40 coupler is recalculated based on H32 data through the regression method, resulting in 23.978 kg-CO2-e/pcs. A total of 70,320 H40 couplers were required for 293 diaphragm wall panels, emitting 1686 tons of carbon emission. Additionally, a total of 23,440 H32 couplers produced 457 tons of carbon emissions.

Subsequently, the total carbon emissions were converted to carbon price by USD 75 per ton of CO_2 [24]. The rebar cost was computed based on the inflation rate [xlvi], resulting in USD 908 per ton of rebar [22]. The material costs and processing costs of rebars and couplers are shown in Appendix A, Table A6. The processing cost is the expense incurred for the installation process of each lap splice or coupler. The processing cost was considered the same for lap splices and couplers. It was calculated to reflect the current inflation rate [46], using the data from the study by Kwon et al. [1]. In addition, a transition coupler is required to connect rebars with different diameters. In this study, the price of the transition coupler required to join H40 and H32 rebars was assumed to be the same as the H40 coupler's price. An amount of USD 868,452 was required to purchase H40 and transition couplers, and USD 197,834 for H32 couplers.

Table 7 summarizes the comparison of the original case and coupler case in terms of rebar quantities, carbon emissions, and associated costs, including rebar cost, coupler cost, processing cost, and carbon price. It has been observed that the proposed algorithm reduced 4053 tons (17.95%) of the purchased rebar quantity from the original case which used only stock length rebars by eliminating lap splices and using couplers instead. A total carbon emissions amount of 12,063 tons (15.24%) were saved. Furthermore, a total cost reduction of USD 3,734,348 (13.91%) was achieved, including rebar cost, labor cost, and carbon price. The processing cost was significantly reduced by USD 215,850 (53.86%).

Table 7. Comparison of the original case and the coupler case in terms of rebar quantities, carbon emissions, and associated costs (293 panels).

Description	Original case (O)	Coupler case (C)	Reduction (O-C)	Reduction rate (O-C)/O
Ordered quantity (ton)	22,582.65	18,529.69	4052.96	17.95%

Preprints (www.preprints.org) | NOT PEER-REVIEWED | Posted: 11 December 2023 doi:10.20944/preprints202312.0703.v1

Carbon emissions (ton)	79,152.19	67,089.54	12,062.64	15.24%
Rebar cost (USD)	20,505,045	16,824,959	3,680,086	17.95%
Coupler cost (USD)	-	1,066,286	-	-
Processing cost (USD)	400,791	184,942	215,850	53.86%
Carbon price (USD)	5,936,414	5,031,716	904,698	15.24%
Overall cost (USD)	26,842,251	23,107,902	3,734,348	13.91%

The costs except the carbon price were converted from KRW to USD using the current exchange rate [46].

Table 8 depicts the comparison between the previous study [15] and the coupler case in terms of rebar usage, carbon emissions, and associated costs. Since the lap splices were substituted by couplers, rebar usage was saved by 1053 tons (5.38%). The overall cost was reduced further by USD 27,646 and the processing cost was further reduced by USD 22,109 (10.68%) from the previous study [15]. This shows that mechanical couplers are significantly effective for the rebar minimization in the case study diaphragm wall, maintaining sustainability in construction.

Table 8. Comparison of the previous case [15] and the coupler case in terms of rebar quantities, carbon emissions and associated costs (293 panels).

Description	Previous case (P)	Coupler case (C)	Reduction (P-C)	Reduction rate (P-C)/P
Ordered quantity (ton)	19,582.36	18,529.69	1052.67	5.38%
Carbon emissions (ton)	68,636.18	67,089.54	1546.63	2.25%
Rebar cost (USD)	17,780,785	16,824,959	955,826	5.38%
Coupler cost (USD)	-	1,066,286	-	-
Processing cost (USD)	207,050	184,942	22,109	10.68%
Carbon price (USD)	5,147,713	5,031,716	115,998	2.25%
Overall cost (USD)	23,135,549	23,107,902	27,646	0.12%

The costs except the carbon price were converted from KRW to USD using the current exchange rate [46].

5. Discussion

Conventional lap splicing is the most common method for rebar connection due to its simplicity and cost-effectiveness. However, it requires adherence to the lapping zone recommended by building codes [17]. Conventional lap splicing is also prone to errors, such as improper lap length or incorrect installation, which can compromise its performance. Additionally, conventional lap splices require more and longer rebar as the diameter increases. ACI [17] prohibits their use for rebar connections larger than 36 mm. Furthermore, lap splices can be difficult to inspect and repair. An alternative to the lap splice is the welded joint or splice method, which consumes less rebar but requires higher costs and skilled labor to execute. However, welded joints emit flames and smoke that could potentially harm surrounding construction works, and the gas used to weld the rebars is not completely environmentally safe. Additionally, welded joints can be vulnerable to cracking if not properly executed.

Conversely, mechanical couplers offer speed and ease of installation, which can save time and costs for construction projects. Mechanical joints enable the connection of adjacent rebars without lapping, requiring less rebar and thus less cutting waste. Additionally, a sharp rise in rebar prices and a shortage of labor have resulted in the increasing use of couplers. Furthermore, the cost of couplers is gradually decreasing over time as their usage becomes more prevalent. Through this study, a 17.95% reduction in rebar usage and a 95.41% in cutting waste was achieved for diaphragm wall structures, demonstrating a near-zero cutting waste. In comparison to the findings of the previous study [15], a further reduction in rebar usage of 5.38% was observed, demonstrating the potential of couplers in promoting accelerated sustainable construction practices.

Despite these benefits, mechanical couplers have not been widely adopted in the construction industry. This is due to a combination of factors, such as the higher initial costs associated with

 doi:10.20944/preprints202312.0703.v1

couplers, the absence of standardized design guidelines for their use, and a general lack of awareness among construction professionals.

A wide variety of couplers are available on the market, some suitable for use in non-seismic regions and others designed to withstand lateral forces. Nevertheless, the selection of the right coupler is crucial to reducing rebar usage, cutting waste, and maintaining structural integrity. Furthermore, couplers are generally only used in new construction, with a few exceptions for retrofitting buildings, where existing reinforcement is already in place. These issues should be addressed in future investigations.

Since couplers are easy to install, they improve construction site productivity. Therefore, couplers require systematic planning and supply chain management (SCM) throughout the construction process to maintain and enhance the productivity of the construction site. Future studies could further explore the planning and development of an SCM strategy that emphasizes couplers, in addition to coupler selection, including the prefabricated rebar cage practices and devices that could be used to aid the prefabricated process. Nonetheless, the broad application of couplers and special length rebars to various construction projects, including buildings, bridges, tunnels, and subways, can significantly reduce rebar usage, saving construction costs, accelerating the construction phase, and reducing the environmental impacts (CO_2 emissions) associated with rebars. Moreover, the reduction of rebar usage and waste aligns with the Sustainable Development Goals (SDGs) proposed by the United Nations, particularly SDGs 12, 13, and 15, which emphasize sustainable production and consumption patterns. This reduction in rebar usage alleviates the environmental burden associated with its production and disposal, contributing to a more sustainable construction industry.

6. Conclusion

This study aims to assess the capabilities of mechanical couplers in optimizing rebar usage in large structural components that require the use of large rebar sizes and improving sustainability with integrated mechanical couplers and a special-length rebar approach. The proposed method was implemented in a case study involving a diaphragm wall reinforced with H32 and H40 diameter rebars. The impact of the proposed method was assessed by comparing its results to those of the conventional lap splices approach. Through this study, several notable findings can be found as follows:

1. The proposed method required 18,530 tons of rebar to be purchased, reducing the rebar usage significantly by 4053 tons (17.95%) compared to the original case with the conventional lap splice approach.
2. The proposed method resulted in a rebar cutting waste rate of 0.57%, presenting the achievement of near-zero cutting waste. The method also reduces the related waste rate by 95.41%.
3. The remarkable impact of the coupler and special-length rebar combination on the environment and construction is demonstrated by the reduction of carbon emissions by 12,063 tons of eCO_2 (15.24%) and a decrease in the total cost by USD 3,734,348 (13.91%) over the original design.
4. Compared to previous findings [15], the rebar usage was further reduced by 1053 tons (5.38%), leading to a reduction in carbon emissions by 1547 tons of eCO_2 (2.25%).
5. These findings highlight the noteworthy capabilities of the couplers and special length rebars combination on exceptionally reducing the rebar usage and rebar cutting waste, contributing to the acceleration of sustainable construction operations, as well as achievement of SDGs. The findings also demonstrate a method for substantially decreasing construction materials, costs, and environmental impact without jeopardizing the structural integrity of diaphragm walls. However, mechanical couplers have not been widely adopted in the construction industry due to several reasons, including the high initial costs and lack of awareness of the engineers and practitioners.

Future investigations should focus on developing systematic planning and supply chain management (SCM) strategies specifically tailored to the integration of couplers and special length rebars, including prefabricated rebar and associated auxiliary devices as these are essential for improving construction site efficiency. This study showcases the potential of the proposed method to significantly reduce rebar usage and cutting waste within a large-scale construction project. Implementing the proposed method across various buildings and infrastructure projects could further multiply these benefits, fostering the rapid adoption of more sustainable and green construction operations.

Author Contributions: Conceptualization, S.K., K.Y.K.; methodology, S.K., K.Y.K.; validation, S.K., D.D.W., L.P.K., K.Y.K.; formal analysis, D.D.W. and L.P.K.; investigation, D.D.W. and L.P.K.; resources, S.K.; data curation, L.P.K.; writing—original draft preparation, D.D.W. and L.P.K.; writing—review and editing, S.K., D.D.W. and L.P.K.; supervision, S.K.; project administration, K.Y.K.; funding acquisition, S.K. All authors have read and agreed to the published version of the manuscript.

Funding: This study was supported by the National Research Foundation of Korea (NRF) grants funded by the Korea government (MOE) (No. 2022R1A2C2005276).

Data Availability Statement: The data that support the findings of this study are available from the corresponding authors upon reasonable request.

Conflicts of Interest: The authors declare no conflicts of interest.

Appendix A

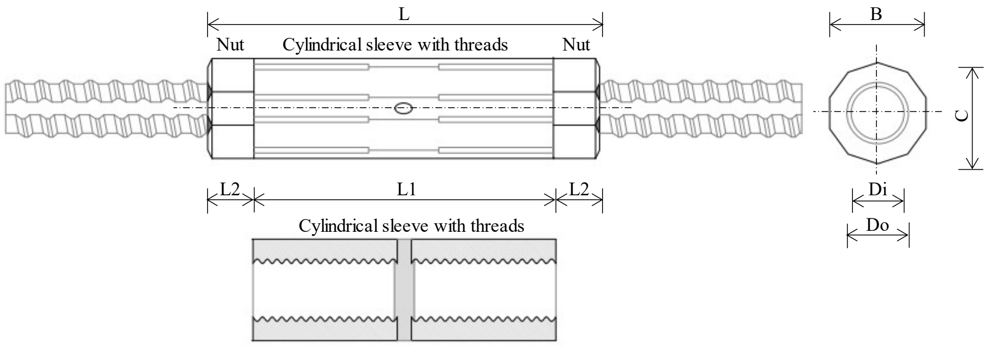

Figure A1. Rib thread coupler details (Tokyo Tekko).

Table A1. Specifications for the rib thread coupler in mm unit (Tokyo Tekko).

Bar Size	Outside diameter of the coupler		Length			Dimension of thread		
			Coupler	Nut	Total	Pitch	Inside diameter	Root diameter
	B	C	L1	L2	L	P	Di	Do
20	31	32.6	110	20	150	8	19.6	23.1
25	40	42.1	140	20	180	10	24.8	29.0
32	50	52.6	190	30	250	13	31.4	36.6
40	64	67.3	220	30	280	16	39.0	45.4

Table A2. Original rebar list of the diaphragm wall.

Serial No.	Description	Bar Mark	Size	No. of Rebar	Length of rebar (m)	Unit weight Kg/m	Total (Kg)	Total (Ton)
1	Main Bars	D2	H40	40	12.000	9.864	4734.720	4.735
2	Main Bars	A2	H40	40	11.425	9.864	4507.848	4.508
3	Main Bars	B2	H40	40	10.775	9.864	4251.384	4.251
4	Main Bars	E2	H40	40	10.775	9.864	4251.384	4.251
5	Main Bars	A1	H40	40	8.865	9.864	3497.774	3.498
6	Main Bars	B1	H40	40	8.865	9.864	3497.774	3.498
7	Main Bars	D1	H40	40	8.865	9.864	3497.774	3.498
8	Main Bars	E1	H40	40	8.865	9.864	3497.774	3.498
9	Main Bars	D3	H40	40	5.665	9.864	2235.182	2.235
10	Main Bars	A3	H32	40	12.000	6.313	3030.240	3.030
11	Main Bars	A4	H32	40	10.560	6.313	2666.611	2.667
12	Main Bars	D4	H32	40	10.560	6.313	2666.611	2.667
13	Main Bars	D3a	H32	40	8.000	6.313	2020.160	2.020
14	Suspension Hook	U1	H40	16	2.750	9.864	434.016	0.434
15	Spacer	S1	H40	58	2.450	9.864	1401.674	1.402
16	Hanging Bar	H1	H40	12	2.450	9.864	290.002	0.290
17	Add'l Lifting Bar	H3	H40	12	2.450	9.864	290.002	0.290
18	Starter Bars	P1c	H40	28	2.160	9.864	596.575	0.597
19	Starter Bars	P2c	H40	4	2.160	9.864	85.225	0.085
20	Starter Bars	P1d	H40	28	2.160	9.864	596.575	0.597
21	Starter Bars	P2d	H40	4	2.160	9.864	85.225	0.085
22	Starter Bars	P1e	H40	24	2.160	9.864	511.350	0.511
23	Starter Bars	P2e	H40	4	2.160	9.864	85.225	0.085
24	Lifting Rebar	H2	H40	16	1.800	9.864	284.083	0.284
25	Starter Bars	G1c	H40	8	1.520	9.864	119.946	0.120
26	Starter Bars	G2c	H40	2	1.520	9.864	29.987	0.030
27	Starter Bars	G1f	H40	28	1.520	9.864	419.812	0.420
28	Starter Bars	G2f	H40	4	1.520	9.864	59.973	0.060
29	Starter Bars	P3c	H32	28	1.570	6.313	277.519	0.278
30	Starter Bars	P4c	H32	4	1.570	6.313	39.646	0.040
31	Add'l vertical bars	C2	H25	40	9.335	3.854	1439.084	1.439
32	Add'l vertical bars	C1	H25	40	5.785	3.854	891.816	0.892
33	Stiffener	L3	H25	44	1.820	3.854	308.628	0.309
34	Starter Bars	P5c	H25	28	1.225	3.854	132.192	0.132
35	Starter Bars	P6c	H25	4	1.225	3.854	18.885	0.019
36	EX-Link	L1	H20	972	4.766	2.470	11,442.403	11.442
37	Fixing Rebar	FR1	H20	16	2.450	2.470	96.824	0.097
38	Starter Bars	G7b	H20	48	0.700	2.470	82.992	0.083
39	Starter Bars	G8b	H20	6	0.700	2.470	10.374	0.010
40	Add'l vertical bars	F1	H20	40	4.320	2.470	426.816	0.427
41	Dowel Bars	SW1	H16	152	1.395	1.580	335.023	0.335
42	Dowel Bars	SW2	H16	76	1.395	1.580	167.512	0.168
43	C-Link	L2	H13	3440	1.214	1.040	4343.206	4.343

Table A3. A new rebar list extracted from the BIM model after applying BS shape codes.

Main Rebars							
Serial No.	**Description**	**Bar Mark**	**Size**	**No. of Rebar**	**Length of rebar**	**Weight (Ton)**	**BS Shape code**
1	Main Bars	D2	H40	40	9.760	3.851	26
2		B2		40	8.535	3.368	26
3		E2		40	8.535	3.368	26
4		A2		40	9.185	3.624	26
5		A1		40	8.865	3.498	00
6		B1		40	8.865	3.498	00
7		D1		40	8.865	3.498	00
8		E1		40	8.865	3.498	00
9		D3		40	3.425	1.351	26
10		A3	H32	40	10.335	2.610	26
11		A4		40	8.895	2.246	26
12		D4		40	8.895	2.246	26
13		D3a		40	6.335	1.600	26
Remaining Rebars							
Serial No.	**Description**	**Bar Mark**	**Size**	**No. of Rebar**	**Length of rebar**	**Weight (Ton)**	**BS Shape code**
1	Suspension Hook	U1	H40	16	2.518	0.397	13
2	Spacer	S1		58	2.450	1.402	00
3	Hanging Bar	H1		12	2.450	0.290	00
4	Add'l Lifting Bar	H3		12	2.450	0.290	00
5	Coupler Bars	P2c		4	2.160	0.085	99-03
6		P2d		4	2.160	0.085	99-03
7		P2e		4	2.160	0.085	99-03
8		P1c		28	2.052	0.567	12
9		P1d		28	2.052	0.567	12
10		P1e		24	2.052	0.486	12
11	Lifting Rebar	H2		16	1.800	0.284	00
12	Coupler Bars	G2c		2	1.520	0.030	99-03
13		G2f		4	1.520	0.060	99-03
14		G1c		8	1.412	0.111	12
15		G1f		28	1.412	0.390	12
16	Coupler Bars	P4c	H32	4	1.570	0.040	99-03
17		P3c		28	1.483	0.262	12
18	Add'l vertical bars	C2	H25	40	8.741	1.348	26
19		C1		40	5.191	0.800	00
20	Stiffener	L3		44	1.820	0.309	26
21	Coupler Bars	P6c		4	1.225	0.019	99-03
22		P5c		28	1.158	0.125	12
23	EX-Link	L1	H20	972	4.766	11.442	99-01
24	Add'l vertical bars	F1		40	4.320	0.427	00
25	Fixing Rebar	FR1		16	2.450	0.097	00
26	Coupler Bars	G7b		48	0.700	0.083	99-04
27		G8b		6	0.700	0.010	99-03
28	Dowel Bars	SW1	H16	152	1.362	0.327	12
29		SW2		76	1.362	0.164	12
30	C-Link	L2	H13	3440	1.214	4.343	99-02

Table A4. Rebar quantities of the original lap splice case (293 panels).

Bar Diameter (mm)	Stock length (m)	No. of rebar	Actual rebar quantity (ton)	Ordered rebar quantity (ton)	Cutting waste (ton)	Loss rate (%)
H40	12	103,136	11,503.56	12,208.00	704.45	5.77%
H32	12	46,880	3135.33	3551.44	416.11	11.72%
H25	12	18,752	817.65	867.24	49.60	5.72%
H20	12	148,258	3533.41	4394.37	860.96	19.59%
H16	12	8497	147.24	161.10	13.86	8.60%
H13	12	112,219	1272.56	1400.49	127.93	9.13%
			20,409.74	22,582.65	2172.91	9.62%

Table A5. Rebar quantities of the previous lap splice case (293 panels) [17].

Description	H40	H32	H25	H20	H16	H13	Total
Required quantity (ton)	12,208.00	3,551.44	867.24	4,394.37	161.10	1,400.49	22,582.65
Ordered quantity (ton)	10,882.29	2,929.94	778.03	3,564.13	144.25	1,283.79	19,582.43
Cutting waste (ton)	1,325.71	621.50	89.21	830.24	16.85	116.71	3000.22
Loss rate (%)	10.9%	17.5%	10.3%	18.9%	10.5%	8.3%	13.3%

Table A6. Material cost and processing cost of rebars and couplers.

Description	Material cost		Processing cost	
	Rebar (USD/ton)	Coupler (USD/pcs)	Lap splice (USD/m)	Coupler (USD/m)
H40	908	12.35	2.09	2.09
H35	908	11.50	1.75	1.75
H32	908	8.44	1.62	1.62
H29	908	6.90	1.32	1.32
H25	908	6.14	1.05	1.05
H22	908	5.37	0.80	0.80
H19	908	4.22	0.59	0.59

The data of H40 was interpolated based on H32 by regression method.

References

1. Kwon, K.; Kim, D.; and Kim, S. Cutting waste minimization of rebar for sustainable structural work: A sy stematic literature review. *Sustainability* **2021**, 13(11), 5929. DOI: 10.3390/su13115929.
2. United States Environmental Protection Agency. Overview of Greenhouse Gases. 2023. Available online: https://www.epa.gov/ghgemissions/overview-greenhouse-gases (accessed on 23 November 2023)
3. Global Cement and Concrete Association. Cement and Concrete around the World. 2023. Available online: https://gccassociation.org/concretefuture/cement-concrete-around-the-world/ (accessed on 23 November 2023)
4. Hanson, J. L.; Manheim, D. C.; Yeşiller, N. Geoenvironmental Assessment of Climate Impacts from Landfill Gas Emissions. *Soils and Foundation* **2023**, 63(2), 101279. DOI: 10.1016/j.sandf.2023.101279.
5. Malmir, T.; Lagos, D.; Eicker, U. Optimization of Landfill Gas Generation based on A Modified First-Order Decay Model: A Case Study in the Province of Quebec, Canada. *Environ Syst Res* **2023**, 12, 6. DOI: 10.1186/s40068-023-00292-w
6. Assadolahfardi, G.; Panahandeh, A.; Khalvati, A.A.; Sekhavati, A. Life cycle assessment of construction phase of monorail project in Qom, Iran. *Pollution* **2017**, 3(1), 81-99. DOI: 10.7508/pj.2017.01.009.
7. Hu, C.; Zhou, Z.; Luo, Y.; Yan, X. Effect of Acid Rain on Mechanical Properties and Aging Mechanism of Asphalt. *J. Mater. Civ. Eng* **2023**, 35(6), 04023137. DOI: 10.1061/JMCEE7.MTENG-14741.
8. Gomes, F.; Brière, R.; Feraille, A.; Habert, G.; Lasvaux, S., Tessier, C. Adaptation of environmental data to national and sectorial context: application for reinforcing steel sold on the French market. *The International Journal of Life Cycle Assessment* **2013**, 18, 926-938. DOI: 10.1007/s11367-013-0558-4.

9. Chen, Y.; Yang, T. Lapping Pattern, Stock Length, and Shop Drawing of Beam Reinforcements of an RC Building. *Journal of Computing in Civil Engineering* **2015**, 29(1), 04014028. DOI: 10.1061/(ASCE)CP.1943-5487.0000303.
10. Nadoushani, Z. S. M.; Hannad, A. W.; Xiao, J.; Akbarnezhad, A. Minimizing cutting wastes of reinforcing steel bars through optimizing lap splicing within reinforced concrete elements. *Construction and Building Materials* **2018**, 185, 600-608, DOI: 10.1016/j.conbuildmat.2018.07.023.
11. Zheng, C.; Yi, C.; Lu, M. Integrated optimization of rebar detailing design and installation planning for waste reduction and productivity improvement. *Automation in Construction* **2019**, 101, 32–47. DOI: 10.1016/j.autcon.2019.01.012.
12. Khondoker, M. T. H. Automated reinforcement trim waste optimization in RC frame structures using building information modeling and mixed integer linear programming. *Automation in Construction* **2021**, 124, DOI: 10.1016/j.autcon.2021.103599.
13. Lee, D.; Son, S.; Kim, D.; Kim, S. Special-Length-Priority Algorithm to Minimize Reinforcing Bar-Cutting Waste for Sustainable Construction. *Sustainability* **2020**, 12, 5950, DOI: 10.3390/su12155950.
14. Widjaja, D. D.; Rachmawati, T. S. N.; Kwon, K.; Kim, S. Investigating Structural Stability and Constructability of Buildings Relative to the Lap Splice Position of Reinforcing Bars. *Journal of The Korea Institute of Building Construction* **2023**, 23(3):315-326, DOI: 10.5345/JKIBC.2023.23.3.315.
15. Rachmawati, T. S. N.; Lwun P. K.; Lim, J.; Lee, J.; Kim, S. Optimization of lap splice positions for near-zero rebar cutting waste in diaphragm walls using special-length-priority algorithms, *Journal of Asian Architecture and Building Engineering* **2023**, DOI: 10.1080/13467581.2023.2278881.
16. Widjaja, D. D.; Kim, S. Reducing rebar cutting waste and rebar usage of beams: A two-stage optimization algorithm. *Buildings* **2023**, 13(9), 2279. DOI: 10.3390/buildings13092279.
17. ACI Committee 318. Building Code Requirements for Structural Concrete (ACI 318-19); and Commentary (ACI 318R-19), Farmington Hills, MI: American Concrete Institute, 2019.
18. Porwal, A.; Hewage, K. N. Building information modeling based analysis to minimize the waste rate of structural reinforcement. *Journal of Construction Engineering and Management* **2012**, 138(8), 943-954, DOI: 10.1061/(ASCE)CO.1943-7862.0000508.
19. Nadoushani, Z. S.; Hammad, A. W. A.; Akbarnezhad, A. A. Framework for Optimizing Lap Splice Positions within Concrete Elements to Minimize Cutting Waste of Steel Bars. Proceedings of the 33rd International Symposium on Automation and Robotics in Construction (ISARC), 2016, Auburn, USA.
20. ugli Makhmudov, J. I. and ugli Sobirov, O. K. SEISMIC RESILIENCE THROUGH DIAPHRAGM WALL CONSTRUCTION. GOLDEN BRAIN, 2023, 1(21), 11-21.
21. Datta, S. D.; Rana, Md. J.; Assafi, M. N.; Mim, N. J.; Ahmed, S. Investigation on the generation of construction wastes in Bangladesh. *International Journal of Construction Management* **2023**, 23(13), 2260-2269. DOI: 10.1080/15623599.2022.2050977.
22. Construction Association of Korea. Construction on hold as material prices go through the roof. Retrieved October 11 2023. https://koreajoongangdaily.joins.com/2022/04/22/business/industry/Inflation/20220422165447730.html
23. Ghayeb, H. H.; Razak, H. A.; Sulong N. H. R. Evaluation of the CO2 emissions of an innovative composite precast concrete structure building frame. *Journal of Cleaner Production* **2020**, 242, 118567. DOI: 10.1016/j.jclepro.2019.118567.
24. IMF. Why countries must cooperate on carbon prices. Retrieved October 11, 2023. https://www.imf.org/en/Blogs/Articles/2022/05/19/blog-why-countries-must-cooperate-on-carbon-prices
25. United Nations Development Programme. The SDGs in Action. 2023. Available online: https://www.undp.org/sustainable-development-goals (accessed on 23 November 2023)
26. Zubaidy, D. S.; Dawood, S. Q.; Khalaf, I. D. Optimal utilization of rebar stock for cutting processes in housing project. *IARJSET* **2016**, 3(5), 189–193. DOI: 10.17148/iarjset.2016.3639.
27. Kim, D.; Lim, C.; Liu, Y.; Kim, S. Automatic Estimation System of Building Frames with Integrated Structural Design Information (AutoES). Iranian Journal of Science and Technology, Transactions of Civil Engineering 2020, 44:1145-1157. DOI: 10.1007/s40996-019-00308-5.
28. Shokrzadeh, M. R.; Nateghi, A. F.; Mansoori, M. R.; Pasha, P. Failure area evaluation of the coupler with threaded bar: Experimental and Numerical study. *International Journal of Advanced Structural Engineering* **2022**, 12(1), 531-543. DOI: 10.1007/IJASE.2022.692294.
29. Bompa, D. V.; Elghazouli, A. Y. Monotonic and cyclic performance of threaded reinforcement splices. *Structures* **2018**, vol. 16, 358-372. DOI: 10.1016/j.istruc.2018.11.009.

30. Nateghi-Alahi, F.; Shokrzadeh, M. R. Behavior considerations for mechanical rebar couplers. In Proceedings of the University of Tokyo International Congress on Science and Engineering, Tokyo, Japan, 14-15 October 2019; pp. 30-41. Available online: https://www.researchgate.net/publication/349772249.
31. Singh, R.; Himanshu, S. K.; Bhalla, N. Reinforcement Couplers As An Alternative To Lap Splices: A Case Study. *International Journal of Engineering Research & Technology* **2013**, 2(2), 1-6. **DOI: 10.17577/IJERTV2IS2542.**
32. Chiari, V. G.; Moreno, J. A. L. Experimental evaluation of coupler behavior for mechanical rebar splices in reinforced concrete structures. *IBRACON Structures and Materials Journal* **2018**, 11, 1326-1353. DOI: 10.1590/S1983-41952018000600009.
33. Damsara, K.D.P.; Kulathunga, D.D.T.K. Analysis on Effectiveness of Rebar Couplers in Splicing of Reinforcement Bars. In Proceedings of International Symposium on Advances in Civil and Environmental Engineering Practices for Sustainable Development (ACEPS-2018), Galle, Sri Lanka, 15 March 2018. Available online: https://www.researchgate.net/publication/325818277_Analysis_on_Effectiveness_of_Rebar_Couplers_in_Splicing_of_Reinforcement_Bars
34. Tazarv, M.; Saiidi, M. S. Seismic design of bridge columns incorporating mechanical bar splices in plastic hinge regions. *Engineering Structures* **2016**, 124, 507-520. DOI: 10.1016/j.engstruct.2016.06.041.
35. Bompa, D. V.; Elghazouli, A. Y. Ductility considerations for mechanical reinforcement couplers. *Structures* **2017**, vol. 12, 115-119. DOI: 10.1016/j.istruc.2017.08.007.
36. Moka, V. T. K.; Rajendran, S. C. Role of coupler in structural behavior of RC elements. Materials Today: Proceedings 2022, 64, 1035-1042. https://doi.org/10.1016/j.matpr.2022.05.097
37. Chidambaram, R. S.; Agarwal, P. Performance evaluation of innovative hybrid rebar coupler in reinforced concrete beams subjected to monotonic loading. *Structural Concrete* **2018**, 19(3), 892-903. DOI: 10.1002/suco.201700083.
38. Qing, Y.; Wang, C. L.; Meng, S.; Zeng, B. Experimental study on the seismic performance of precast concrete columns with thread-bolt combination couplers. *Engineering Structures* **2022**, 251, 113461. DOI: 10.1016/j.engstruct.2021.113461.
39. Yousheng, D., Keqin, Z., Wenjie, L., Qian, S., & Erli, M. Optimization of beam parameters for coupling beam pile structure foundations under vertical loading. *The Structural Design of Tall and Special Buildings* **2023**, 32(5-6), e2007.
40. Mironov, D. A., Osokin, A. I., Loseva, E. S., & Kuzhelev, A. I. Specific features of diaphragm wall construction. *In IOP Conference Series: Materials Science and Engineering* **2020**, Vol. 775, No. 1, p. 012051. IOP Publishing.
41. Alsakka, F.; Haddad, A.; Ezzedine, F.; Salami, G.; Dabaghi, M.; Hamzeh, F. Generative design for more economical and environmentally sustainable reinforced concrete structures. *Journal of Cleaner Production* **2023**, 387, 135829.
42. Proposed Reinforced Pre-assembly Method for Tokyo Steel Co., Ltd. Presentation.
43. Tokyo Tekko Company Ltd., Threaded Rebar Joint, ACE-Joint. https://www.tokyotekko.co.jp/en/prd/tekko/nsts/nsts04/main/04/teaserItems1/0/linkList/0/link/31.Catalogue_Ace-Joint.pdf (accessed on 23 November 2023)
44. Tokyo Tekko Company Ltd., Neji-Tetsu-Con (Hot rolled threaded rebar). Available online: https://www.tokyotekko.co.jp/en/prd/tekko/tc/tc01/main/03/teaserItems1/00/linkList/0/link/30.Catalogue_Neji-Tetsu-Con.pdf (accessed on 23 November 2023)
45. Tokyo Tekko Company Ltd., Neji-Tetsu-Con (Hot rolled threaded rebar). Available online: https://www.tokyotekko.co.jp/en/prd/tekko/tc/tc01/main/03/teaserItems1/00/linkList/0/link/30.Catalogue_Neji-Tetsu-Con.pdf (accessed on 23 November 2023)
46. World Economic Outlook, Navigating Global Divergences, October 2023. Available online: https://www.imf.org/en/Publications/WEO/Issues/2023/10/10/world-economic-outlook-october-2023 (accessed on 23 November 2023)